Mesoscale Modeling of Hydrogen Embrittlement in Iron-Hydrogen Alloys

Daniel L. Coelho[1], **Nikolas Provatas**[1]

[1]Department of Physics, Center for the Physics of Materials, McGill University, Montreal, Quebec, Canada H3A 2T8

daniel.coelho@mail.mcgill.ca

1. Introduction

Hydrogen embrittlement (HE) is the loss of ductility and strength in metals such as iron (Fe) and steel alloys due to the absorption of hydrogen atoms (H). Grain boundaries (GBs) act as sinks for hydrogen, making these materials more susceptible to void initiation and propagation, which can ultimately lead to failure.

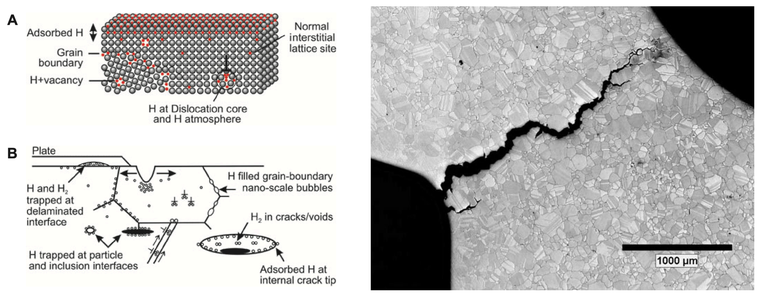

Fig. 1: Schematic illustrations of sites and traps for hydrogen in materials on the (a) atomic, and (b) microscopic scale (left). An example of brittle fracture due to HE [1] (right).

HE poses a significant risk in engineering applications, as exposure to hydrogen can compromise the integrity of certain metals. This can lead to hydrogen leaks, structural failures, and even fires. Proper material selection, alloy design, and protective measures are essential to mitigate these risks. Although experimental studies have improved our understanding of HE, the relationship between solutes in GBs and HE remains unclear, and a unified theory bridging atomic-scale mechanisms and mesoscale microstructure is still lacking [2].

Here, we investigate the atomistic mechanisms of HE by simulating the segregation of H in Fe GBs using a **Phase-field crystal** (PFC) approach [3].

2. Objectives

- Simulate hydrogen segregation in iron grain boundaries using an extended two-component PFC model and analyze its impact on void formation over diffusive time scales;
- Examine the influence of hydrogen on grain boundary energy.

3. Methodology

1) Binary Phase Field Crystal Model

We employ the PFC approach developed in Ref. [4] for modeling phase transformations in solid-liquid-vapor systems through the use of higher-order direct correlations. This was extended to a binary (A-B) system with the free energy functional formulated as follows,

$$\begin{aligned}\Delta\bar{F} = \tau \int d\mathbf{r}\Big\{ &\tfrac{1}{2}C_0(\tau)n_A^2 - \tfrac{1}{6}D_0 n_A^3 + \tfrac{1}{12}E_0 n_A^4 + \tfrac{1}{2}n_A\big(C_{AA}^{(2)} * n'_A\big) \\ &- \tfrac{1}{6}D_2(\tau)n_A\big(C_{AA}^{(3)} * n'_A\big)^2 + \tfrac{1}{12}E_3(\tau)n_A\big(C_{AA}^{(4)} * n'_A\big)^3 \\ &+ n_A\big(C_{AB}^{(2)} * n'_B\big) + \tfrac{1}{2}n_B^2 - \tfrac{1}{6}n_B^3 + \tfrac{1}{12}n_B^4 + \tfrac{1}{2}n_B\big(C_{BB}^{(2)} * n'_B\big)\Big\} \end{aligned} \quad (1)$$

where $\Delta\bar{F} \equiv \Delta F[n_A, n_B]/k_B T_0 \rho_0 a_0^d$, and $n_i(\mathbf{r}) = (\rho_i(\mathbf{r}) - \rho_0^i)/\rho_0^i$ measures the local microscopic density relative to a reference density (ρ_0^i) for each species ($A \equiv$ Fe and $B \equiv$ H). The density fields are governed by *conserved* dynamics,

$$\partial_t n_i = M_i \nabla^2 \mu_i \,, \quad (2)$$

where $\mu_i = \delta\Delta\bar{F}/\delta n_i$ is chemical potential and M_i is the mobility of species i, for $i = A, B$.

3. Methodology [cont.]

2) Two-particle Interactions

The interactions between Fe and H atoms are modeled using two-point direct correlation functions, formulated in Fourier space as,

$$C_{ij}^{(m)}(k) = A_{ij}^{(m)} e^{-\frac{k^2}{2\beta^2}} + B_{ij}^{x} e^{-\frac{T}{T_0}} e^{-\frac{(k-k_0)^2}{2\alpha^2}} \quad (3)$$

where $k_0 = 2\pi/a_0$ is the dominant reciprocal lattice wave-vector of the crystal structure, and $\exp(-\tau)$ controls temperature dependence of the correlation peaks, where $\tau = T/T_0$.

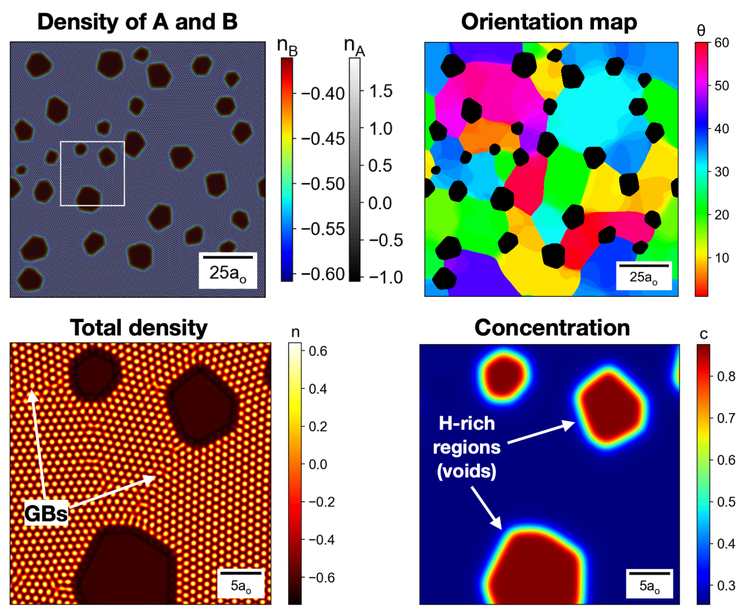

Fig. 2: Void formation in polycrystalline PFC iron at $T = 300$ K. Concentration shown is $c = (\bar{n}_B + 1)/(\bar{n}_A + \bar{n}_B + 2)$, where the total density is $\bar{n} = (\bar{n}_a + \bar{n}_B)/2$.

3) Equilibrium Properties of the Fe-H system

In the present study, we model iron (A species) in two dimensions using the two-point correlation of a triangular-forming lattice. Hydrogen (B species) is assumed to be an ideal gas and interacts on long-wavelengths with iron. We coarse-grain the miscroscopic free energy functional onto a smooth free energy function as follows

$$\underbrace{\Delta\bar{F}[n_A, n_B]}_{\text{Microscopic free energy}} \longrightarrow \underbrace{\Delta\bar{F}[\bar{n}_A, \bar{n}_B] \quad \text{or} \quad \Delta\bar{F}[\bar{n}, c]}_{\text{Smooth free energy in } (\bar{n}_A, \bar{n}_B) \text{ or } (\bar{n}, c) \text{ representations}} \quad (4)$$

where $\bar{n}_A$ and $\bar{n}_B$ are the average densities of species A and B, respectively. We define the concentration to be $c = (\bar{n}_B+1)/(\bar{n}_A+\bar{n}_B+2)$, where the total density is $\bar{n} = (\bar{n}_a + \bar{n}_B)/2$.

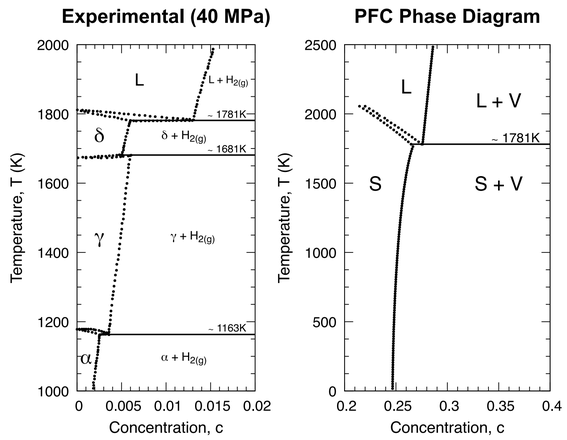

Fig. 3: Experimental Fe-H phase diagram adapted from Ref. [5] (left), and the PFC phase diagram (right).

4. Grain boundary energy

We examined the scenario of an equal tilt bicrystal in coexistence with the vapor phase, for a single misorientation angle and different H concentrations.

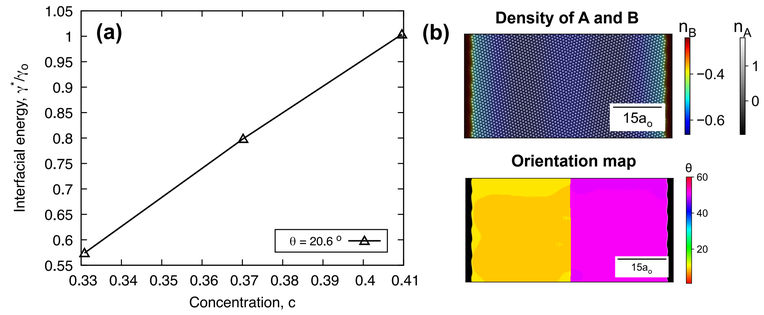

Fig. 4: (a) Dimensionless interfacial energy of a PFC bicrystal as a function of H concentration at a fixed temperature of $T = 300$ K. (b) Example of a PFC bicrystal with a tilt angle of $\theta = 20.6^o$.

5. Nanovoid Formation and Growth

We also simulated H-charging of a PFC bicrystal coexisting with the vapor phase by introducing a spatially dependent flux in the chemical potential of B species, $\mu_B \rightarrow \mu_B + \mathcal{S}_B$. This flux is applied only on the surrounding vapor phase.

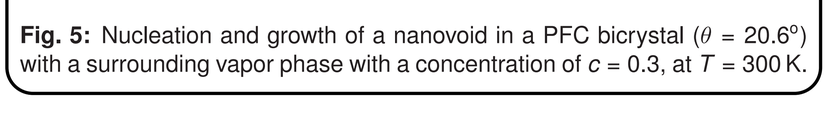

Fig. 5: Nucleation and growth of a nanovoid in a PFC bicrystal ($\theta = 20.6^o$) with a surrounding vapor phase with a concentration of $c = 0.3$, at $T = 300$ K.

6. Discussion and Future Work

We examined the microstructure evolution guided by the phase diagram of the proposed model. Our numerical results demonstrate that hydrogen destabilizes the microstructure by increasing grain boundary (GB) energy. The higher interfacial energy cost makes GBs more susceptible to instability, ultimately promoting void formation along GBs.

Future work:

- Incorporate higher k peaks in the direct correlation functions to simulate a wider range of crystal structures in the solid part of the phase diagram;
- Verify Sievert's law for solid-gas adsorption effects ($c_{\text{dissolved}} = K\sqrt{P_{H_2}}$);
- Perfom stress analysis during tensile tests of polycrystals to examine the impact of hydrogen concentration on yield strength.

7. References

[1] M. Iannuzzi, A. Barnoush, and R. Johnsen, "Materials and corrosion trends in offshore and subsea oil and gas production," *npj Materials Degradation*, vol. 1, no. 1, p. 2, 2017.

[2] O. Barrera, D. Bombac, Y. Chen, T. D. Daff, E. Galindo-Nava, P. Gong, D. Haley, R. Horton, I. Katzarov, J. R. Kermode, *et al.*, "Understanding and mitigating hydrogen embrittlement of steels: a review of experimental, modelling and design progress from atomistic to continuum," *Journal of Materials Science*, vol. 53, no. 9, pp. 6251–6290, 2018.

[3] K. R. Elder, M. Katakowski, M. Haataja, and M. Grant, "Modeling elasticity in crystal growth," *Phys. Rev. Lett.*, vol. 88, no. 24, p. 245701, Jun. 2002.

[4] D. L. Coelho, D. Burns, E. Wilson, and N. Provatas, "Generalizing the structural phase field crystal approach for modeling solid-liquid-vapor phase transformations in pure materials," *Physical Review Materials*, vol. 8, no. 9, p. 093402, 2024.

[5] A. San-Martin and F. D. Manchester, "The Fe-H (iron-hydrogen) system," *Bulletin of Alloy Phase Diagrams*, vol. 11, no. 2, pp. 173–184, 1990.